Article

Frequency-Shift of Quartz Crystal Microbalance Depends on the Length of Actin Filaments

Naoki Matsumoto[1], Honoka Kobayashi[1], Taiki Nishimura[1], Hideki Ashizawa[3], Takashi Kuwahara[1,2], Hajime Honda[1,2] and Ikuko Fujiwara[1,2*]

[1] Department of Bioengineering, Nagaoka University of Technology, Niigata, Japan
[2] Department of Materials Science and Bioengineering, Nagaoka University of Technology, Niigata, Japan
[3] RIVER ELETEC CORPORATION, 2-1-11 Fujimigaoka, Nirasaki, Yamanashi 407-8502, Japan
* Correspondence: ikukofujiwara@vos.nagaokaut.ac.jp

Abstract: Quartz Crystal Microbalance (QCM) is a well-known method to measure the mass of ligands bound to receptor-covered surfaces in various fields, ranging from materials science to biology. Actin molecule is essential in various cellular processes through its function of monomer-to-filament polymerization, forming a double-stranded filament with a 75 nm pitch. In this study, QCM was applied to measure the physical properties of actin, finding that the frequency shifted negatively when monomeric actin bound to the QCM surface, whereas the frequency shifted positively when filaments bound. Using fluorescence light microscopic observations, we have examined whether negative and positive frequency shifts originated from their length. In order to control this process, a severing protein, fragmin was used to change the length of actin filament. When the average length of filaments shortened, the magnitude of positive shift decreased in a concentration-dependent manner. However, shorter filaments showed a negative frequency shift depending on their concentration, showing that the weight derived from the loaded concentration and the function derived from actin polymerization dynamics are detectable. Interestingly, the transition from positive to negative occurred when the average length of actin was ~33 nm, or approximately equal to the half-pitch of filaments. Thus, actin filaments can serve as an excellent standard to measure the mechanical properties of biopolymers. Our results show that the QCM sensor could be both a "weight" and a "function" sensor of biomolecules in vitro.

Keywords: quartz crystal microbalance; actin; positive frequency shift; physical property; biomolecule

1. Introduction

The Quartz Crystal Microbalance (QCM) is an acoustic wave device. QCM can detect the mass weight and mechanical properties of substances bound to the QCM-electrode as a negative shift of resonance frequency, which is proportional to the mass of the substance. An equation represents the relationship between the bound substance and its mass [1], enabling us to measure various binding reactions of ligand-receptor interactions in the real-time, including gas, humidity, bacteria, and protein-protein interactions [2-5]. In liquid phase measurements, QCMs exhibit different frequency shifts in the presence of substances [6, 7] because this device is sensitive to the viscoelastic properties of the tested samples and buffers. While these properties of samples and buffer conditions limit the use of QCM in liquid, some researchers have used QCM as an immune sensor and successfully measured cell adhesion by signals immobilized on the electrode surface [4]. This study reported positive frequency shifts that deviated from Sauerbrey's behavior [8]. This positive frequency shift is triggered independently from the dissociation of the substrate from the electrode and is mainly affected by the substance's adsorption kinetics and viscoelastic properties.

Preprints (www.preprints.org) | NOT PEER-REVIEWED | Posted: 3 May 2023 doi:10.20944/preprints202305.0114.v1

Actin has a molecular mass of 42 kDa and is one of the most abundant proteins in eukaryotic cells. It drives cell motility, including cell protrusion, migration, divisions, and more, mainly because it is located immediately beneath the plasma membrane of living cells. Actin generates force by polymerizing, forming a double-stranded filament (F-actin) with a 7 nm diameter [9-11] that drives cell motility. This polymerization function can be visualized by conjugating fluorescent dyes at the level of individual filaments, in which one end (called the barbed end) polymerizes and depolymerizes much faster than the other end (called the pointed-end) when observed under total internal reflection fluorescence microscopy [12]. The polymerization dynamics are regulated by over one hundred types of actin-associated factors to facilitate cell functions. Some of the regulatory factors are gelsolin, ADF/cofilin in eukaryotes, and fragmin in the slime mold Physarum polycephalum, severing F-actin by binding the side of the filament to accelerate the turnover of the actin cytoskeleton in living cells, inhibiting further polymerization by capping the barbed-end, and increasing the amount of F-actin for rapid response during cell motility [13]. During cell motility, mechanical stress is relayed through the cytoplasm to the actin cytoskeleton. Applying physical stress is a powerful approach to studying cells' mechanical properties and responses. Atomic Force Microscopy (AFM) and optical trapping can be applied to detect spatiotemporal mechanical forces via probes that are directly attached to the cell membrane and proteins. However, these forces are applied to a minimal and confined area and might not be strong enough to monitor viscoelastic changes in the intracellular actin cytoskeleton and cytoplasm.

In this study, QCM was used to monitor the mechanical property of biopolymer. When we applied actin as a biopolymer, the frequency shifted negatively when monomeric actin (G-actin) was bound to the QCM electrode surface, but the shift became positive when F-actin bound. The magnitude of this positive frequency shift decreased as the average length of F-actin decreased, suggesting that F-actin is an excellent control for measuring bio-sample heterogeneity based on size. Interestingly, under our experimental conditions, positive- and negative-frequency transitions occurred when the average length of F-actin was between 36 and 55 nm (i.e., when the molar ratio of fragmin to actin was between 1:19 and 1:14), corresponding to the half-pitch of F-actin. These observations suggest that molecules in the cytoplasm might contribute to the propagation of external stimuli by their presence, in addition to their binding to specific partners.

2. Materials and Methods

2.1. Proteins

Actin was prepared from an acetone powder of rabbit skeletal muscle following one cycle of polymerization and depolymerization [14]. It was stored on ice in buffer G (2 mM Tris, pH 8.0, 0.2 mM ATP, 0.1 mM $CaCl_2$, 0.5 mM dithiothreitol (DTT)). Actin concentration was determined by absorbance using an extinction coefficient of $\varepsilon_{290} = 0.0266$ / μM / cm_2. The cation bound to G-actin was converted from Ca^{2+} to Mg^{2+} by adding buffer F (final 25 mM Tris-HCl (pH 8.0), 25 mM KCl, 1 mM EGTA, 4 mM $MgCl_2$) to polymerize a 500 μL volume of 1.6 μM actin. After 30 min incubation at 25°C, 9 μL of 100 μM TRITC-Phalloidin (P1951-1MG) dissolved in dimethyl sulfoxide (~1.1 times the actin concentration for a sufficient amount) was mixed with F-actin in buffer F and stored in the dark on ice.

P. polycephalum Fragmin was genetically engineered into the expression vector pGEX-6P-1 (GE Healthcare, Japan) [15]. The recombinant fragmin was expressed in Escherichia coli BL21 (DE3) cells (Thermo Fisher Scientific Inc.) and was affinity-purified using a glutathione resin. After the N-terminal glutathione S-transferase (GST)-tag was removed by precision protease, fragmin was further purified on a gel filtration column (Sephacryl S200 16/60; GE Healthcare) equilibrated with A-buffer (2 mM Tris–HCl (pH 7.5), 0.5 mM EGTA, 1 mM DTT). The concentration was determined using an extinction coefficient of $\varepsilon_{280} = 0.0454$ / μM / cm. Severed F-actin was prepared by mixing 1000 nM TRITC-Ph-F-actin with different concentrations of fragmin (final 0, 2.8, 36, 333, and 500 nM) in the A buffer containing 0.2 mM $CaCl_2$ for 5 min at 25°C.

Preprints (www.preprints.org) | NOT PEER-REVIEWED | Posted: 3 May 2023 doi:10.20944/preprints202305.0114.v1

Since actin takes both monomeric and filamentous forms through its polymerization function, non-polymerizable G-actin was prepared by conjugating a fluorescence dye on cysteine 374 of actin and prevented F-actin [16]. Unpolymerized actin was prepared using 2 ml of 40 μM G-actin after removing DTT by dialysis against DTT-free G buffer for 24 h at 4°C. After polymerizing actin by adding final 100 mM KCl and 2 mM $MgCl_2$, 20 μL of 100 mM tetramethylrhodamine-5-maleimide (TMR) dissolved in N,N-dimethylformamide was quickly and vigorously mixed with F-actin. The mixture of F-actin and TMR was incubated in an end-to-end rotor for 18~24 h at 4°C. After centrifugation at 29,000 x g for 90 min at 12°C (CS 100GXL, Eppendorf Himac Technologies, Japan), the labeled F-actin was collected as a pellet and suspended in 1 mL of G-buffer. The suspended TMR-actin was further dialyzed against G-buffer for 24 h at 4°C in the dark, and free dye was removed with a disposable column (PD MidiTrap G-25, GE Healthcare Bio Sciences AB, Sweden). Extinction coefficients of $\varepsilon 290 = 0.0266$ / μM / cm and $\varepsilon_{550} = 0.0969$ / μM / cm were used. The typical labeling ratio was ~80% [12]. Actin was incubated with final 100 mM KCl and 2 mM MgCl2 for 30 min at 23°C in the dark, followed by centrifugation at 29,000 x g for 90 min at 12°C. Finally, the supernatant was collected as the unpolymerized fraction [16].

2.2. QCM chip and glass preparation

The QCM chips were AT-cut crystal devices specially ordered and produced by RIVER ELETEC CORPORATION (fundamental frequency F_0, 16 MHz), and some of them were coated with SiO_2 prepared by sputtering.

In advance of coating glasses with 3-aminopropyltriethoxysilane (APTES), QCM chips were thoroughly cleaned with a basic Piranha solution (30% H2O2 and NH_4OH in 3:7 (v/v) mixture) for 20 min. The electrode was pretreated with 2-mercaptethanol to create -OH groups on the surface. No pretreatment was carried out for the SiO_2-covered electrode. For cleaning larger coverslip glasses (24 × 50 mm; Matsunami Glass Ind., Ltd. Osaka, Japan, Neo No. 1) on the opposite side of the electrode, acidic Piranha solution (30% H_2O_2 and concentrated H_2SO_4 in 3:7 (v/v) mixture) was added for 10 min. Both glasses were rinsed with deionized water [17, 18]. Following all pretreatments, the surface of dried QCM chips was immersed in 2% of APTES in absolute EtOH, and the surface of the coverslip glass was covered with 2% hexamethyldisilazane for 8 h. After immersion, both types of QCM chips and glasses were rinsed with absolute EtOH, then placed in deionized water [5]. Chips and glasses were thoroughly dried in a clean chamber for 1 h before use.

2.3. Flow chamber preparation

Flow chambers were prepared daily by mounting a QCM chip on the glass placed with two double-sided tapes of 0.1 mm thickness (ST415 25 × 30, 3M, Japan) in parallel, leaving a gap of ~5 mm. The size of the flow chamber was approximately 15 × 5 × 0.1 mm with both sides open (~10 μl volume). A copper tape was placed on both sides of the QCM device and pasted using conductive paste.

2.4. Measurement

The resonant frequency of QCM for SiO_2-coated devices was performed using a crystal oscillator (SUNRISE INDUSTRIAL CO., LTD, QSRX-1504N 27-21-2) with a 12 V supply (KIKUSUI ELECTRONICS CORP, MODEL PAB 32-0.5) and a frequency counter (HP Japan, HEWLETT 53132A). For non-SiO_2-coated devices, measurements were performed using a network analyzer (HP Japan, E5100A). The output was recorded on a PC every minute in both measurements.

2.5. Specimens

Before loading solutions in the flow chamber, the A-buffer was loaded directly into the chamber via a capillary action every 3 min until resonance frequency stabilized and the fluctuation range of the measured value was within 5 Hz. Excess buffer was absorbed from the opposite side using cut-off pieces of coffee filter paper for rapid absorption. Sample solution of either F- or unpolymerized

 doi:10.20944/preprints202305.0114.v1

G-actin was loaded every 3 or 6 min, respectively, on the chamber consisting of SiO_2-coated QCM chips connected with the network analyzer.

2.6. Microscopic Observations and image analysis

TRITC-Ph-F-actin was visualized with a fluorescence light microscope (Olympus IX-73, Japan). A mercury lamp was used to excite the fluorophores, and a camera (HAMAMATSU, DIGITAL CAMERA C11440) connected to a computer was used to record images. A built-in filter cube (Olympus, U-MWIG) was used as a set of excitation and emission filters with a dichroic mirror.

2.7. Image analysis

The average length of TRITC-Ph-F-actin in control was estimated from 20 F-actin filaments by using ImageJ (https://imagej.nih.gov/ij/download.html). The average length of F-actin in the presence of fragmin was estimated by dividing the length of control F-actin by the added-fragmin concentration.

3. Results

3.1. QCM frequency shifts by G- and F-actin

Frequency shift was investigated by immobilizing actin to APTES-coated QCM electrodes. To measure binding, $\Delta F=F-F_0$ was plotted after each surface treatment. Figures 1A and 1B represent typical frequency shift profiles measured from either G- or F-actin binding. The shift in frequency decreased over time after loading various concentrations of G-actin (Fig. 1A). Plateaus of frequency shift was low after increasing the concentrations of loaded TMR-G-actin (Fig. 1C, circles), confirming that this assay detects a surface-bound protein in a concentration-dependent manner. The frequency shift increased after F-actin loading, when measuring the shift by F-actin. G-actin contamination was prevented by decollating F-actin with TRITC phalloidin (TRITC-Ph-F-actin or F-actin) [19]. Phalloidin minimizes the amount of G-actin by stabilizing actin as F-actin due to its tight binding affinity. We confirmed that TRITC-Ph-F-actin was bound to the surface using a fluorescent microscope (Fig. 1C). While the frequency gradually decreased over time, the plateau of frequency shift was still positive. However, this result showed that the fractions of positive frequency shift increased in proportion to the concentration of F-actin (Fig. 1D), implying that the physical property, such as forms of the protein, dynamically changes the frequency shift from negative to positive.

Preprints (www.preprints.org) | NOT PEER-REVIEWED | Posted: 3 May 2023 doi:10.20944/preprints202305.0114.v1

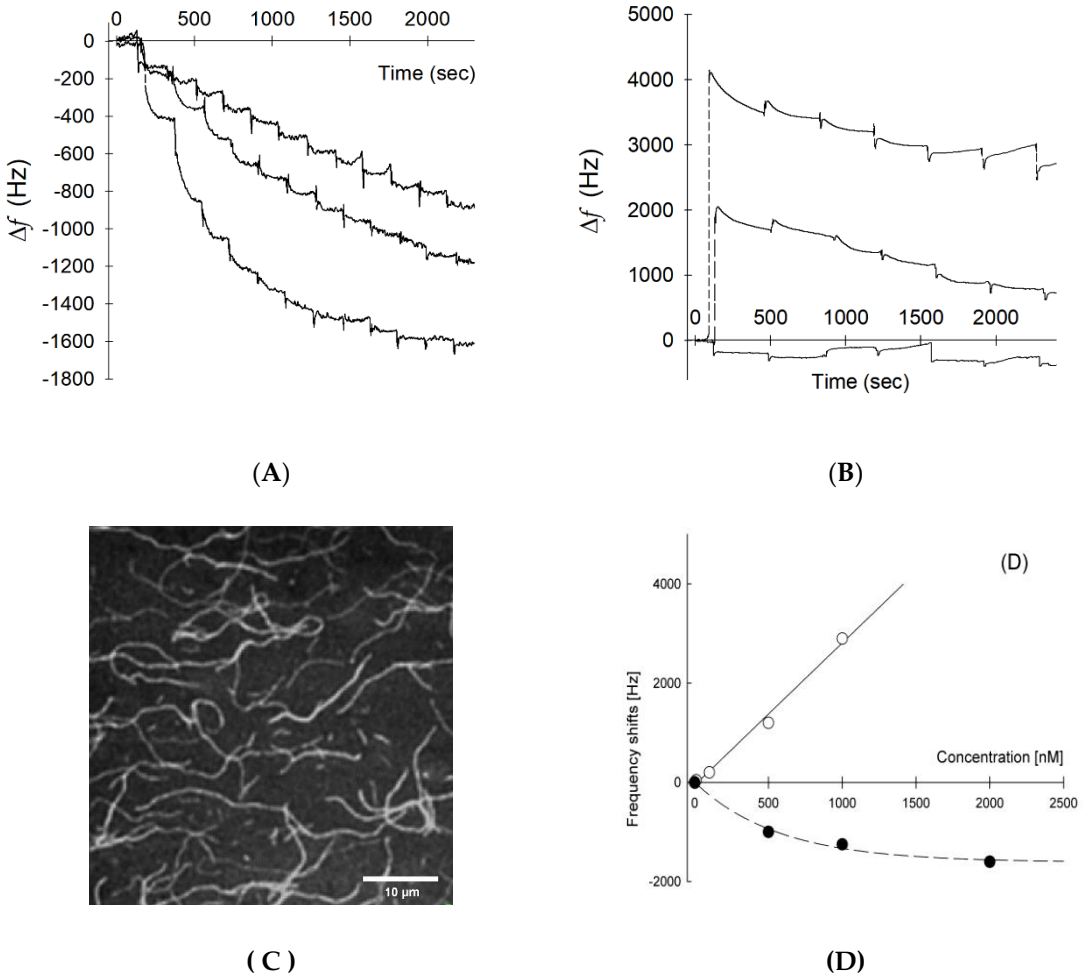

Figure 1. Frequency changes by loading G- or F-actin: (A) Time course of frequency shift when loading 500, 1000, and 2000 nM (upper, middle, and bottom lines, respectively) of G-actin (unpolymerized by chemical modification) into the chamber every 3 min. (B) ΔF change when loading 1.0, 500, and 1000 nM (bottom, middle and upper lines, respectively) of F-actin into the chamber every 6 min. (C) Fluorescence micrograph of 1000 nM TRITC-Ph-F-actin absorbed on the QCM electrode surface. The scale bar is 10 μm. (D) Plot of the summary of panels (A) and (B), i.e., concentration dependence of the frequency shifts by loading G-actin (filled circles) and F-actin (open circles).

3.2. The frequency shift and length of filaments

Fragmin was employed to investigate whether the positive frequency shift depends on sample heterogeneity based on size (Fig. 2A). Fragmin is a severing protein of F-actin and remains on the barbed end in the presence of Ca2+. Under a constant concentration of actin (1000 nM), the frequency shift was positive when fragmin concentration was low. However, it became negative under high fragmin concentrations (Fig. 2C). Light microscopy confirmed that fragmin shortened the length of F-actin (Fig. 2B). A high concentration of fragmin (Fig. 2D) bound to the surface was caused by only a ~100 Hz decrease in frequency shift, much smaller than the shift using severed F-actin. This result indicates that the frequency shift was not derived from the bound fragmin on the QCM electrode surface. Our data showed that the frequency shift was positive when the average length of F-actin was long, but it became negative when F-actin was short, suggesting that the length of TRITC-Ph-F-actin is a crucial factor in switching the frequency shift from negative to positive. We note that the length of TRITC-Ph-F-actin was estimated from the molar ratio of fragmin over actin by assuming that all fragmin binds to actin. At a 0.1 ratio, we assumed that fragmin binds to F-actin containing 10 actin molecules. F-actin is a double-stranded filament having a 36 nm half pitch, in where 13 actin molecules are included [11]. The plot of the frequency shift over the estimated length of TRITC-Ph-

Preprints (www.preprints.org) | NOT PEER-REVIEWED | Posted: 3 May 2023 doi:10.20944/preprints202305.0114.v1

F-actin showed that the switch in shift occurred when the filament was ~33 nm long, similar to a half pitch of F-actin.

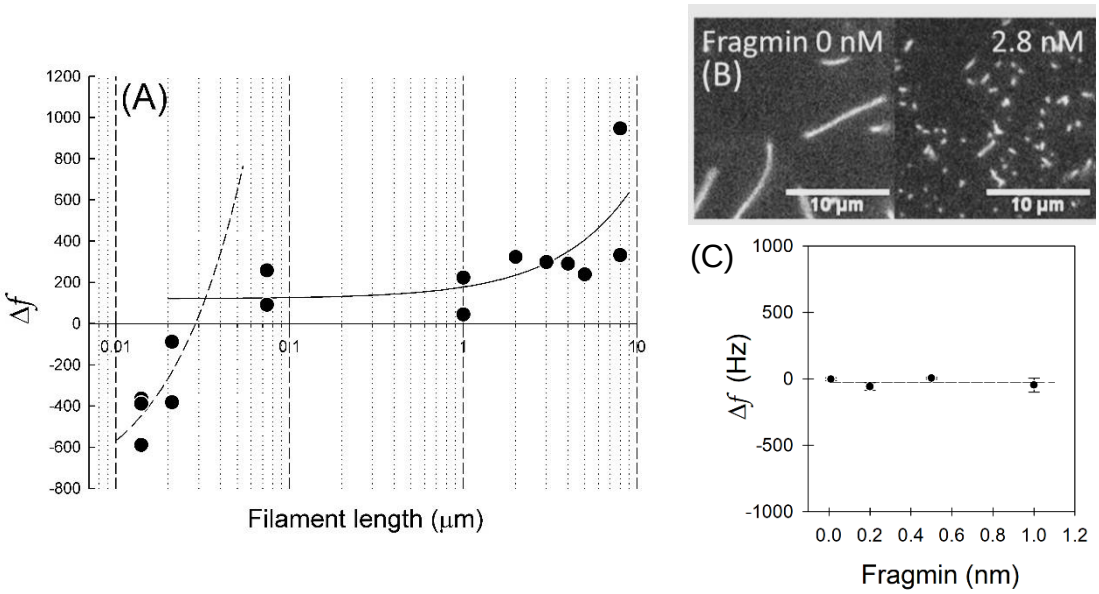

Figure 2. Frequency change by loading different lengths of F-actin: Length-controlled filaments were prepared by mixing 1000 nM F-actin with varying concentrations of fragmin and incubating for 5 min at 25°C. (A) Frequency change vs. F-actin length calculated from the ratios and size of actin. Solid and broken lines represent linear fittings of positive and negative shift data. Two lines intersected when length was about 33 nm. (B) Fluorescence images of severed F-actin in the presence of 0 and 2.8 nM fragmin. Scale bars are 10 μm. (C) Frequency changes by fragmin in the absence of actin molecules. A broken line indicates the linear fitting.

4. Discussion

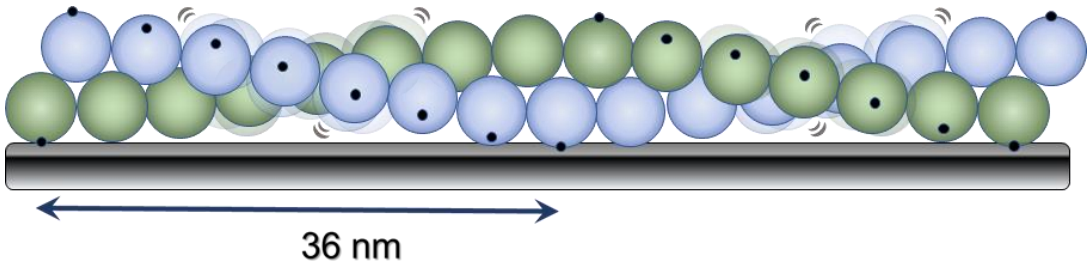

Figure 3. Schematic drawing of the attachment of biopolymer having a double-helix with half a pitch of 36 nm on the QCM electrode: Blue and green spheres represent the monomers in each strand of biopolymer. Black spheres indicate the electrostatically plausible points of attachment of each subunit. The grey plane beneath the biopolymer represents the electrode surface.

One of the biopolymers, filamentous actin demonstrated a positive frequency shift on the QCM electrode in our experiment, even though monomeric actin showed negative frequency shift. In this report, we carefully manipulated solution exchanges to minimize share stress using a classic light conventional microscopic technique often used during in vitro motility assays of actomyosin, and combined it with hand-made QCM measurement systems. The flow in our experiment was mild slow enough to maintain the length of F-actin at more than several tens of micrometers (see Fig.1C), while

 doi:10.20944/preprints202305.0114.v1

in a conventional QCM measurement with non-manual solution exchange system, the flow may be too fast and disrupt the supramolecular structures of molecules functioning in living cells. The actin-binding protein, fragmin, was used to control the length of the filament. Fragmin is known to attach to the barbed end of a filament, thereby avoiding further elongation. Although F-actin can be observed under a fluorescence microscope, very short filaments, i.e., less than ca. 500 nm, cannot be measured due to the limitation of the spatial resolution. Thus, we calculated filament length based on a mixing ratio of fragmin/actin. As a result, filaments less than about 33 nm in length demonstrated a negative frequency shift, called Sauerbrey effect whereas longer filaments displayed a positive frequency shift, called anti- Sauerbrey effect. This length of a F-actin may be closely related to its double-helical structure, having a half-helical pitch size of 36 nm.

Why were the positive shifts proportional to the concentration, i.e. weight of the actin molecule? Although the persistent length of is long of ~16.7 μm [20, 21], F-actin is not so easy to be bent in transversal directions [22]. In contrast, F-actin can be twisted easily in a standard aqueous solution [23, 24]. If we consider a semiflexible polymer that possesses the mechanical properties as described above and assume that it is fixed to the electrode's surface at particular locations via electrostatic attachment, it is likely that the next plausible attachment point for the double-stranded polymer on the QCM surface would be half a pitch distance from the initial point (Fig. 3). Repeat of this "unit of attachment" could bring a proportional increase in frequency shift. If the length of the polymer is less than half of a pitch, it may be possible to achieve a relatively strong binding to the electrode if the twisting the biopolymer, resulting in the typical negative frequency shift of QCM.

5. Conclusions

We demonstrated that a frequency shift of QCM by actin filaments changes from negative to positive occurred at about 33 nm, and that the magnitude of frequency shift was proportional to the weight or concentration of the molecules. Our results indicate that this simple QCM method could measure physical changes of biological supra-molecules, such as actin filaments, in vitro. Of significance, filamentous proteins, which often exist in a helical form, may present a positive frequency shift in a weight- or concentration-dependent manner. These findings suggest that the QCM sensor can serve not only as a "weight sensor" but also as a "function sensor" of biomolecules.

Author Contributions: The experiment was designed by NM, HH, and IF. NM, TN, HA, JO, TK, HH, and IF prepared samples and the experimental setup, collected experimental data, and conducted the analyses. NM, HH, and IF wrote the manuscript. All the authors approved the final version of the manuscript.

Funding: This study was supported by the Research Foundation of Opto-Science and Technology to IF, the Nagaoka University of Technology Strategic Research Grant 2021 to IF, and JSPS KAKENHI Grant Number JP20K06591.

Institutional Review Board Statement: The study was conducted in accordance with the Declaration of Helsinki. The Institutional Ethics Committee of Nagaoka Univ approved the animal study protocol (Tech. No. R2-6).

Acknowledgments: We thank Dr. Shuichi Takeda in Research Institute for Interdisciplinary Science (RIIS), Okayama University, Okayama for the kind gift of the fragmin. Furthermore, we thank Dr. Koichi Takimoto in Department of Materials Science and Bioengineering, Nagaoka University of Technology, Niigata and Mr. Junji Oshita for the helpful discussion about this experiment and all lab members for helpful discussion and technical assistance with protein purification.

Conflicts of Interest: The authors declare no conflicts of interest.

References

1. Sauerbrey, G., Verwendung von schwingquarzen zur wagung dunner schichten und zur mikrowagung. *Zeitschrift fur Physik A Hadrons and Nuclei* **1959,** 155, (2), 206-222.
2. Sun, P.; Jiang, Y.; Xie, G.; Du, X.; Hu, J., A room temperature supramolecular-based quartz crystal microbalance (QCM) methane gas sensor. *Sensors and Actuators B: Chemical* **2009,** 141, (1), 104-108.
3. Erol, A.; Okur, S.; Yağmurcukardeş, N.; Arıkan, M. Ç., Humidity-sensing properties of a ZnO nanowire film as measured with a QCM. *Sensors and Actuators B: Chemical* **2011,** 152, (1), 115-120.

 doi:10.20944/preprints202305.0114.v1

4. Olsson, A. L.; Van der Mei, H. C.; Busscher, H. J.; Sharma, P. K., Influence of cell surface appendages on the bacterium− substratum interface measured real-time using QCM-D. *Langmuir* **2009,** 25, (3), 1627-1632.
5. Albet-Torres, N.; O'Mahony, J.; Charlton, C.; Balaz, M.; Lisboa, P.; Aastrup, T.; Månsson, A.; Nicholls, I. A., Mode of heavy meromyosin adsorption and motor function correlated with surface hydrophobicity and charge. *Langmuir* **2007,** 23, (22), 11147-11156.
6. Kanazawa, K. K.; Gordon II, J. G., The oscillation frequency of a quartz resonator in contact with liquid. *Analytica Chimica Acta* **1985,** 175, 99-105.
7. Furusawa, H.; Ozeki, T.; Morita, M.; Okahata, Y., Added mass effect on immobilizations of proteins on a 27 MHz quartz crystal microbalance in aqueous solution. *Analytical Chemistry* **2009,** 81, (6), 2268-2273.
8. Latif, U.; Can, S.; Hayden, O.; Grillberger, P.; Dickert, F. L., Sauerbrey and anti-Sauerbrey behavioral studies in QCM sensors—Detection of bioanalytes. *Sensors and Actuators B: Chemical* **2013,** 176, 825-830.
9. Fujii, T.; Iwane, A. H.; Yanagida, T.; Namba, K., Direct visualization of secondary structures of F-actin by electron cryomicroscopy. *Nature* **2010,** 467, (7316), 724-728.
10. Murakami, K.; Yumoto, F.; Ohki, S. Y.; Yasunaga, T.; Tanokura, M.; Wakabayashi, T., Structural basis for Ca^{2+}-regulated muscle relaxation at interaction sites of troponin with actin and tropomyosin. *Journal of Molecular Biology* **2005,** 352, (1), 178-201.
11. Oda, T.; Iwasa, M.; Aihara, T.; Maéda, Y.; Narita, A., The nature of the globular-to fibrous-actin transition. *Nature* **2009,** 457, (7228), 441-445.
12. Fujiwara, I.; Takahashi, S.; Tadakuma, H.; Funatsu, T.; Ishiwata, S. i., Microscopic analysis of polymerization dynamics with individual actin filaments. *Nature Cell Biology* **2002,** 4, (9), 666-673.
13. Kinosian, H. J.; Selden, L. A.; Estes, J. E.; Gershman, L. C., Kinetics of gelsolin interaction with phalloidin-stabilized F-actin. Rate constants for binding and severing. *Biochemistry* **1996,** 35, (51), 16550-16556.
14. Spudich, J. A.; Watt, S., The regulation of rabbit skeletal muscle contraction I. Biochemical studies of the interaction of the tropomyosin-troponin complex with actin and the proteolytic fragments of myosin. *Journal of Biological Chemistry* **1971,** 246, (15), 4866-4871.
15. Kanematsu, Y.; Narita, A.; Oda, T.; Koike, R.; Ota, M.; Takano, Y.; Moritsugu, K.; Fujiwara, I.; Tanaka, K.; Komatsu, H., Structures and mechanisms of actin ATP hydrolysis. *Proceedings of the National Academy of Sciences USA* **2022,** 119, (43), e2122641119.
16. Otterbein, L. R.; Graceffa, P.; Dominguez, R., The crystal structure of uncomplexed actin in the ADP state. *Science* **2001,** 293, (5530), 708-711.
17. Corso, C. D.; Stubbs, D. D.; Lee, S.-H.; Goggins, M.; Hruban, R. H.; Hunt, W. D., Real-time detection of mesothelin in pancreatic cancer cell line supernatant using an acoustic wave immunosensor. *Cancer Detection and Prevention* **2006,** 30, (2), 180-187.
18. Nazarov, D. V.; Zemtsova, E. G.; Solokhin, A. Y.; Valiev, R. Z.; Smirnov, V. M., Modification of the surface topography and composition of ultrafine and coarse grained titanium by chemical etching. *Nanomaterials* **2017,** 7, (1), 15.
19. Lengsfeld, A. M.; Löw, I.; Wieland, T.; Dancker, P.; Hasselbach, W., Interaction of phalloidin with actin. *Proceedings of the National Academy of Sciences USA* **1974,** 71, (7), 2803-2807.
20. Ott, A.; Magnasco, M.; Simon, A.; Libchaber, A., Measurement of the persistence length of polymerized actin using fluorescence microscopy. *Physical Review E* **1993,** 48, (3), R1642.
21. Yasuda, R.; Miyata, H.; Kinosita Jr, K., Direct measurement of the torsional rigidity of single actin filaments. *Journal of Molecular Biology* **1996,** 263, (2), 227-236.
22. Arai Y., Yasuda R., Akashi K., Harada Y., Miyata H., Kinosita Jr, K., Itoh, H. Tying a molecular knot with optical tweezers. *Nature* **1999,** 399 (6735). 446-448
23. Egelman, E.; Francis, N.; DeRosier, D., F-actin is a helix with a random variable twist. *Nature* **1982,** 298, (5870), 131-135.
24. Gittes, F.; MacKintosh, F., Dynamic shear modulus of a semiflexible polymer network. *Physical Review E* **1998,** 58, (2), R1241.